Research Repository UCD

Provided by the author(s) and University College Dublin Library in accordance with publisher policies., Please cite the published version when available.

| | |
|---|---|
| ***Title*** | Estimation of structural parameters using static loading tests |
| ***Authors(s)*** | Covián, E.; Casero, M.; González, Arturo |
| ***Publication date*** | 2013-06-20 |
| ***Conference details*** | 11th International Conference on Structural Safety and Reliability (ICOSSAR 2013), Columbia University, New York, USA, 16-20 June 2013 |
| ***Link to online version*** | http://icossar2013.org/ |
| ***Item record/more information*** | http://hdl.handle.net/10197/6539 |

Downloaded 2019-03-24T07:33:40Z

The UCD community has made this article openly available. Please share how this access benefits you. Your story matters! (@ucd_oa)

Some rights reserved. For more information, please see the item record link above.

# Estimation of structural parameters using static loading tests

E. Covián & M. Casero

*Escuela Politécnica de Mieres, Universidad de Oviedo, Asturias, Spain*

A. González

*School of Civil, Structural and Environmental Engineering, University College Dublin, Dublin Co., Ireland*

ABSTRACT: The increasing stock of aging infrastructure demands new convenient and efficient methods for early damage detection. In this paper, focus is placed upon methods that use static measurements via modern surveying techniques. Theoretical simulations play an important role in the development of damage detection methods. These simulations use noise-free data or corrupt the ideal response with noise to resemble a field scenario. However, the nature and true uncertainty of the measured structural response is commonly ignored. Here, the uncertainty associated to modern surveying techniques employed for measuring deflections and rotations is quantified and used to propose site-specific noise models. The latter are used to assess the accuracy of a Cross-Entropy static damage detection algorithm.

## 1 INTRODUCTION

An increasing number of large structures are approaching the end of their design life, while others may have been built based on wrong assumptions (i.e., traffic flows underestimated in bridges), which could represent an aging acceleration factor. Health monitoring of these structures is required to ensure their safety. There is now technology to live-monitor characteristics of a structure such as acceleration, deflection, rotation, strain and temperature and to provide an accurate image of the structure's health. However, this monitoring is often overlooked for many structures due to cost and design/installation complications. Therefore, there is a need for a convenient and efficient method of monitoring, so that damage can be detected sooner and propagation minimized. This paper focuses on damage detection techniques based on static measurements, and how the number of measured points (*measurement density*) and the uncertainty of these measurements affect the accuracy of these techniques.

For a given load, the static response is related to the boundary conditions and distribution of structural stiffness throughout the structure. As damage can be characterized as a local reduction in structural stiffness, analysis of the structure's static response has been used extensively to locate and quantify damage (Sanayei & Scampoli, 1991; Hjelmstad & Shin, 1997; Bakhtiari-Nejad et al., 2005; Caddemi & Morassi, 2007, Walsh & Gonzalez 2009 and Yang & Sun, 2010). Most of these methods use a finite element (FE) mathematical model as reference, and deflections and rotations as inputs. However, these inputs need to be measured and "no measurement is ever exact" (Ghilani & Wolf, 2006). In order to address the later, preliminary theoretical testing of new algorithms may pollute the ideal structural responses with random errors in an attempt to simulate a more realistic scenario. However, these simulated errors are not in agreement with

their own nature, and their uncertainty for a particular confidence level is commonly ignored.

Although previous researchers (Marchamalo et al. 2011; de Luis, 2009; Gordon & Lichti, 2007; Olalla, 2007; Psimoulis et al. 2006; Li et al. 2006; Boehler & Marbs, 2004; Mills & Barber, 2004 and Cheng et al. 2002) have investigated the accuracy of measurements for many techniques, this accuracy has often been expressed as nominal values or referred to observable measurands (as opposed to objective measurands), and as a result, the suggested values are not comparable. In this paper, the uncertainty associated to modern surveying instruments and techniques, such as programmable and reflector-less total station and terrestrial laser-scanner is quantified. Then, noise models are proposed for simulating different field scenarios. Finally, the impact of measurement uncertainty and *measurement density* on a static damage detection algorithm is assessed using theoretical simulations corrupted with the noise models.

## 2 DAMAGE DETECTION METHODS

### 2.1 *General Overview*

Damage detection methods can be classified in two main groups: those that subject the structure to static loading and those that use measurements from dynamic test data. A third category could be considered for those methods that combine both static and dynamic test data.

The main differences between both approaches are: i) equations of dynamic equilibrium depend on mass, damping and stiffness matrix whereas equations of static equilibrium depend solely on the stiffness matrix; ii) High order of modal data, as well as certain mode shapes, that are needed in some dynamic methods, can be difficult to obtain; iii) In static methods, damage at certain locations of the structure can be concealed due to load paths associated with the load applied. The latter reflects the importance of adequately choosing the applied load as well as the need for a parameter that would help to make that choice (Bakhtiari-Nejad et al. 2005; Yang & Sun, 2010).

A review on dynamic based methods can be found in Yan et al. (2007), while an example of a method combining both static and dynamic data is provided by Wang et al. (2001). This paper focuses on static based methods and how measurement uncertainty can affect their performance.

### 2.2 *Damage Detection Methods based on static test data*

Sanayei & Scampoli (1991) propose a method to calculate structural parameters from a subset of degrees of freedom, for which displacement measurements have been taken, by minimizing the error resulting from the comparison between two stiffness matrix (analytical and measured). They analyse the acceptable level of error in the measurements to maintain the input/output error relationship in the linear range. Once established, they conduct a simulation performing probabilistic parameter identification with different subsets of parameters and affecting measurements by the error previously calculated. Hjelmstad & Shin (1997) develop a static parameter estimation algorithm that includes an adaptive parameter grouping scheme in order to deal with sparse data. Hjelmstad and Shin use the output error proposed by Banan et al. (1994), which is defined as the difference between computed and measured displacements. In addition, a measured data perturbation scheme is presented, where estimated parameters are considered as random variables and two damage indices (calculated using the mean and standard deviation of their distributions) are introduced.

Bakhtiari-Nejad et al. (2005) introduce an algorithm based on the comparison of the load vectors of the damaged and undamaged structure. An error vector is formulated as the difference between both load vectors and then a minimization problem is stated subjected to two constraints: a non-linear equality that reflects the measured change in displacement and an inequality ensuring negative change in stiffness.

Moreover, they include selection criteria for load cases, baseline values and measurements locations. The measurements error is found to have no effect on the algorithm performance. Nevertheless, no particular noise treatment is proposed. Caddemi & Morassi (2007) develop closed-form expressions for the determination of the location and magnitude of cracks in beams, subjected to different boundary conditions (pinned-pinned, pinned-clamped and clamped-free). Cracks are modelled as rotationary springs of constant related to the severity of the damage. The accuracy of the estimated crack location is found to decrease significantly for low levels of damage.

Yang & Sun (2010) approach the problem of locating and quantifying damage in a decoupled fashion. The flexibility disassembly theory is used as the location algorithm, obtaining a damage location vector that identifies the damaged elements. Then, damage is quantified for those elements through a perturbed stiffness parameter. Abdo (2011) conducts a parametric study of the relationship between damage and displacement curvature. He states that damage represents a discontinuity in the curvature that can be located and quantified using Grey system theory to compare the curvature of damaged and undamaged structures. Measurement noise is found to have a negligible effect on the results.

Walsh & González (2009) apply cross-entropy (CE) to damage detection. They develop an iterative algorithm that creates a certain number of trial beams and selects those with a deflection similar to the one measured. Then, based on the statistics of the selected best trial beams, a new sample is generated and the process is repeated until convergence is achieved. Noise treatment and its influence on the algorithm performance are yet to be explored. In a further section, the performance of this CE algorithm is tested in the presence of field-like noisy measurements. Regarding the measurement errors, the usual approach, when a numerical simulation is performed, is to consider an "artificial" random noise to simulate real measurements. This noise is expressed as a percentage of the computed or analytical value (examples in the literature range from 0,002% to 10%). However, it would be interesting to choose the magnitude of the noise in relation to the precision of the measurement device used in the field. This simulation will fulfil the purpose of testing the algorithm in realistic conditions.

## 3 ACCURACCY OF SURVEYING TECHNIQUES

### 3.1 *Principles in deflection and rotation measurements*

One of the goals of this paper is to determine if the accuracy associated to a measurement technique is sufficient to guarantee the correct performance of the CE static damage detection algorithm mentioned in Section 2.2. Deflections and rotations are the inputs used on this algorithm and reflector-less electronic tachymeter (TAC) and terrestrial laser-scanner (TLS), commonly referred to as *high definition survey* (HDS), the measurement instruments selected. Deflection and rotation are indirectly measured, since observable measurands are acquired firstly and then a model is applied to calculate them.

As in every measurement, many error sources bring differences between the true values and measures of a particular measurand (BIMP, 2012). The nature of known error sources should be analysed and procedures applied to reduce the error, in order to reach goodness of measures. These procedures are focused, firstly, on eliminating gross and systematic error components and, then, on minimizing random error component in measurements (Covián & Puente, 2013).

Here, the stages of instrument calibration, atmospheric corrections and, in the case of tachymeter, Bessel compensation are supposed to be applied to reduce systematic errors. The most unfavourable combination of random error sources is considered when quantifying, in pre-analysis, the accuracy of a given instrumentation (see Sections 3.2 and 3.3). Pre-analysis error estimations are propagated in order to calculate the

final error of the objective measurands —defections and rotations—.

Finally the value of the measurand ($x$) should be expressed, in accordance with *Guide to the expression of uncertainty in measurement* (BIMP, 2008), showing not only the reference value of the measurand but also its uncertainty and associated confidence level:

$$x = \bar{x} \pm U_x = \bar{x} \pm k \times s_x \quad (1)$$

where $\bar{x}$ is the reference value, $U_x$ is the uncertainty, $\sigma_x$ is standard deviation of the measurand and $k$ is a coverage factor ($k > 1$) that depends on the selected probability distribution. In accordance with the *Bureau International des Poids et Mesures* recommendations (BIMP, 2008), 95% of confidence level ($k = 1.96$) of the normal distribution is adopted here.

Previous research has reported on the accuracy of different measurement techniques. Some (Marchamalo et al. 2011; Olalla, 2007; and others) mention precision data as the nominal value given by the manufacturers, in accordance or not with ISO rules, and referred to observable but not to objective measurand. Recent investigations on differential GPS (Marchamalo et al. 2011; Cheng et al. 2002; Psimoulis et al. 2006; Li et al. 2006 and others) are carried out in large scale structures (breakwaters, suspension bridges and skyscrapers) characterized by being slender and flexible structures with large displacements. While some research on HDS try to determine precision through comparison with reference values of point positions in laboratory (short distances) (Gordon & Lichti, 2007 and Boehler & Marbs, 2004), others try to do it in real scenarios (long distances) comparing results to other techniques (de Luis, 2009 and Mills & Barber, 2004). Generally, HDS real scenarios show precisions unable to capture deflections smaller than 15 mm accurately.

### 3.2 *Surveying techniques to measure deflection*

Both techniques —TAC and HDS— are based on the same observational measurands and relational models in order to determine the deflections ($u_i$) in many points ($i$ = 1, 2… $n$) distributed along a beam (Fig. 1). In Figure 1, A and B are the supports of the beam under investigation (solid thick line represents the initial position and solid dashed line represents the $l_j$ loading case), E is the location of the measurement instrument and $a_i$ is the height of the instrument. $x^E y^E z^E$ and $x^A y^A z^A$ are the axes of the reference systems for the measurement instrument and for the beam analysis, respectively. Therefore, it is necessary to apply a *Helmert transformation* to go from measured data to structural data, in which the ordinate $y$ becomes the same for all the points. The observational measurands are: geometrical distance between the origin of the measurement instrument and the viewed point ($d_g$) and horizontal ($\theta$) and zenithal ($\lambda$) angles. These measurands are considered for the first position of every point ($P_i^0$) corresponding to the initial condition of the structure and for a second position ($P_i^{l_j}$) resulting from applying a loading case ($\forall j = 1, 2 \ldots m$).

While TAC is more accurate than HDS, the latter measures much more points (higher *density*) than TAC. The next two equations show the relation between observable measurands and the deflection (Eq. 2) and between the estimated errors of observable measurands and the error of the deflection (Eq. 3):

$$u_i = d_g^0 \times \cos \lambda^0 - d_g^{l_j} \times \cos \lambda^{l_j} \quad (2)$$

$$s_{u_i} = 2 \times \sqrt{s_{d_g}^2 \times \cos^2 \lambda^0 + s_\lambda^2 \times \left(d_g^0 \sin \lambda^0\right)^2} \quad (3)$$

where $d_g^0$, $d_g^{l_j}$, $\lambda^0$ and $\lambda^{l_j}$ are described above, and $s_{u_i}, s_{d_g}, s_\lambda$ are the estimated errors of deflections, geometrical distances and zenithal angles, respectively. Equation 2 can be deduced from Figure 1, and Equation 3 comes from the application of variance-covariance propagation law (Ghilani & Wolf, 2006). Equation 3 has been obtained considering no variation between the first ($P_i^0$) and the second position ($P_i^{l_j}$) of every point,

since the effect of this assumption in deflection error ($s_{u_i}$) is negligible.

Prior to the resolution of Equation 3, it is necessary to establish the estimated errors of observable measurands: geometric distance error ($s_{d_g}$) and zenithal angle error ($s_{\prime}$), which can be calculated using Equations 4, 5:

$$s_{d_g} = a + b(\text{ppm}) \times d_g \quad (4)$$

$$s_{\prime} = \sqrt{\left(s_{comp}/3\right)^2 + s_{ang}^2} \quad (5)$$

where $a$ (usually expressed in mm) and $b$ (in ppm), determined in accordance with ISO 17123-3 (ISO, 2001), are the error component derived from the phase-meter precision and the error derived from the instability of the wavelength of the EDM system respectively (Covián & Puente, 2013); $\sigma_{comp}$ is the precision of the vertical compensator and $\sigma_{ang}$ is the angular error component in accordance with ISO 17123-4 (ISO, 2001). This info is generally specified in the equipment datasheets for $k$ = 1 (68,26 % of confidence level), so this is too for the geometric distance error ($s_{d_g}$) and for zenithal angle error ($s_{\prime}$).

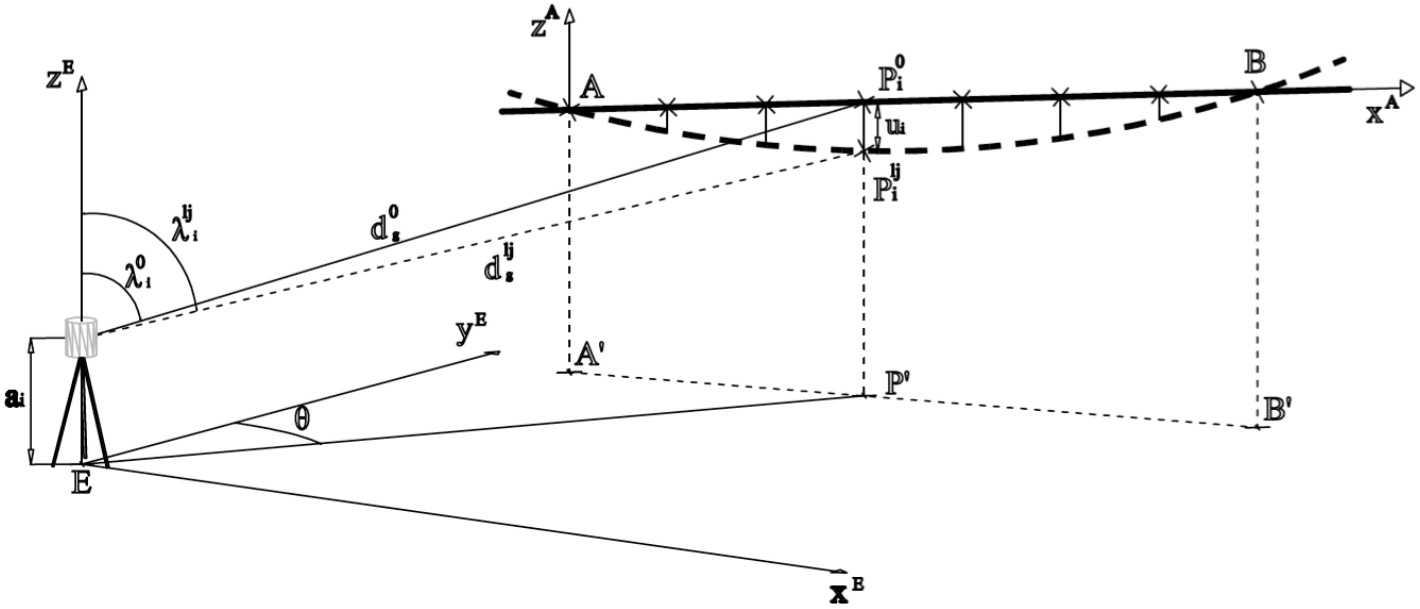


Figure 1. Deflection measurement: reference systems, observable and objective measurands.

### 3.3 *Surveying techniques to measure rotation*

The determination of the rotations of each section of the beam between two different load states ($\rho_i$), through surveying measurements, require to measure the position of two reflectors, situated in the superior and inferior flanges of the beam, in both load states.

Applying the same principles as in Section 3.2, the estimated error of the rotations ($\sigma_\rho$) is:

$$s_r = 2 \times \arctan \frac{\max\left(s_{x_P}, s_{z_P}\right)}{d¢/2} \quad (6)$$

where $s_{x_P}, s_{z_P}$ are estimated errors of the abscise and *applicate* (z-coordinate) or height, respectively; and *d'* is the distance between reflector centres.

## 4 NUMERICAL SIMULATIONS

### 4.1 *Cross-Entropy algorithm for estimation of structural stiffness from static measurements*

Given the distribution of flexural stiffness (modulus of elasticity x inertia) of a beam of known boundary conditions and fixed static loading conditions, its deflection profile is unique. In the in-

verse problem consisting of a limited number of available displacements (possibly corrupted), a number of stiffness distributions may be able to reproduce these displacements. The CE algorithm relies on a FE model to establish the global stiffness matrix of the beam, the latter being function of the flexural stiffness of each discretized FE and its length. The CE method proposes an iterative procedure where a number of FE trial beams (TBs) are generated based on stiffness values that are randomly sampled from a predefined statistical distribution (i.e., normal) of mean and standard deviation updated in each iteration. Thus, a different set of TBs with different stiffness profiles and, consequently, different deflection profiles, is obtained at each iteration of the algorithm. In particular, a total of 1000 TBs are generated in each iteration in this paper. The deflection of each TB is compared against that of the true beam and those TBs performing best (lowest mean square error of the deflections at measured points) are selected to update statistical distributions associated to each discretized beam element for the next iteration. In this paper, the best 10% of all TBs are retained. The process is repeated until the rate of change of error of the objective function (sum of the squared differences between target/measured deflections and predicted deflections using FE model for each observation point) falls below 0.01% over 10 iterations. Then, injection (artificial widening of the statistical distribution) is applied to prevent the algorithm falling into local minima. This injection is repeated for three convergences of the algorithm. Values for the initial statistical distributions of flexural stiffness for each discretized FE are random, although the mean is selected to be within expected theoretical values and the standard deviation is set at 20% of the mean value. Further details can be found in Walsh & González (2009).

### 4.2 *Theoretical scenarios for testing*

A simply supported beam, of span length 21 m, is used to test the performance of the algorithm. A flexural stiffness of 3450 MN·m$^2$, typical of a 21 m bridge, is adopted. In all cases, the applied loads consist of a uniformly distributed load (equivalent to the self-weight of the bridge deck) and two concentrated loads of 10 t each separated by 5 m and located symmetrically with respect to midspan (simulating 2-axle truck). Vertical deflections are simulated at every node of the FE model. Displacements from points within 2 m from the supports are not used as inputs to the algorithm. These displacements near supports are ignored because they are small and of order of magnitude similar to the expected noise, increasing computational without necessarily improving the results.

While HDS allows measuring a point every 1 mm (100 elements/m), such a high number of elements increases the computational time in excess, and a measurement density of 50 displacements/m is adopted here for the HDS equipment. A measurement density of 10 displacements/m is assumed to simulate data gathered by TAC equipment. Two discretization levels are considered for the FE beam, 10 and 50 elements/m, to facilitate the implementation of the algorithm when providing TAC and HDS measurements respectively. In addition, the same stiffness value is assigned to all the elements contained within one meter to speed up calculations, instead of considering an individualized value for each discretized element.

Four case scenarios are considered for both TAC and HDS data: (i) noise-free measurements from healthy beam, (ii) noisy measurements from healthy beam, (iii) noise-free measurements from damaged beam, and (iv) noisy measurements from damaged beam. Damage is modelled as a 40% stiffness reduction between 12 m and 13 m. As such a sudden drop in stiffness is not likely in a real situation, a 10% stiffness reduction is applied in adjacent meters to smooth the stiffness profile.

### 4.3 *Noise model*

The nominal accuracies of the selected instruments (table 1) that have any influence in the deflection errors are:

Table 1. Nominal accuracies for *Leica TCRP1201* tachymeter and Leica ScanStation2 laser-scanner.

| | TAC (Leica TCRP1201) | HDS (Leica ScanStation2) |
|---|---|---|
| **distance accuracy** ($s_{dg}$) | 2 mm + 2 ppm · $d_g$ [1] | 4 mm [2] |
| **angular accuracy** ($s_{ang}$) | 1" [1] | 60 mrad = 12,38" |
| **compensator accuracy** ($s_{comp}$) | 0.5" | 1" |

All the accuracies correspond to one sigma (k = 1).
[1] According with ISO 17123-3 and ISO17123-4.
[2] Out of rules and at a 0 - 50 m range.

Maximum deflection errors, estimated in the pre-analysis (see Section 3.1), at a 95% of confidence level, are shown in table 2 for TAC and HDS following application of Equations 3, 4, 5. They are given for combinations of horizontal distances and heights of the target points with respect to the measurement instrument. For the theoretical testing in the section that follows, a 6 m high bridge is assumed (relevant values are in bold in table 2). It is also assumed that the station is located at an optimal distance that minimizes the quadratic sum of the deflection errors along the beam. Finally, the theoretical deflections that result from the beam model in Section 4.2 are contaminated using an additive noise model (i.e., adding a value randomly sampled from a statistical distribution modelling noise to the true deflection). The noise model is given by a normal distribution of mean zero and a standard deviation that depends on the geometrical distance from each measurement point to the station.

Table 2. Deflection errors for *Leica TCRP1201* tachymeter and Leica ScanStation2 laser-scanner in many probable observation conditions.

| $s_{ui,\,TAC,\,95\,\%}$ (mm) | | $d_{HZ}$ (horizontal distance in m) | | |
|---|---|---|---|---|
| | | 15,00 | 21,00 | 30,00 |
| h (height in m) | 0,00 | 0,289 | 0,405 | 0,578 |
| | 3,00 | 1,588 | 1,202 | 0,990 |
| | 6,00 | 2,973 | **2,238** | 1,687 |
| | 9,00 | 4,114 | 3,185 | 2,394 |
| | 12,00 | 5,000 | 4,004 | 3,061 |
| | 15,00 | 5,669 | 4,692 | 3,669 |
| $s_{ui,\,HDS,\,95\,\%}$ (mm) | | horizontal distance (m) | | |
| | | 15,00 | 21,00 | 30,00 |
| height (m) | 0,00 | 3,529 | 4,941 | 7,058 |
| | 3,00 | 4,681 | 5,416 | 7,229 |
| | 6,00 | 6,809 | **6,555** | 7,699 |
| | 9,00 | 8,805 | 7,910 | 8,374 |
| | 12,00 | 10,411 | 9,216 | 9,151 |
| | 15,00 | 11,635 | 10,367 | 9,949 |

## 5 THEORETICAL TESTING

### 5.1 *Noise-free simulations*

When deflection measurements are noise-free, the CE algorithm is reliable in both no damage and damage situations for the load and structural model under investigation (Section 4.2). The estimated stiffness profiles are consistent with the expected targets and able to capture the localised loss of stiffness (Fig. 2). The estimated peak loss of stiffness is relatively smaller and spread over a slightly wider length than the target value. However, the overall loss of stiffness and critical location where it occurs, are correctly identified.

The difference in stiffness profiles shown in Figure 2 for different runs of the CE algorithm (i.e., test1, test2, test3, test4 and test5 in the figure) is a result of the random nature of the sampling through each iteration (Section 4.1). The uncertainty associated to the nature of the algorithm can be reduced by using an average of a number of CE tests as shown in the figure. Therefore, the 'average' curve is the closest curve to the target profile in the figure. Figures 2a, b are obtained using measurements every 10 cm along beam and Figures 2c, d are obtained using measurements every 2 cm (excluding 2 m at each end support).

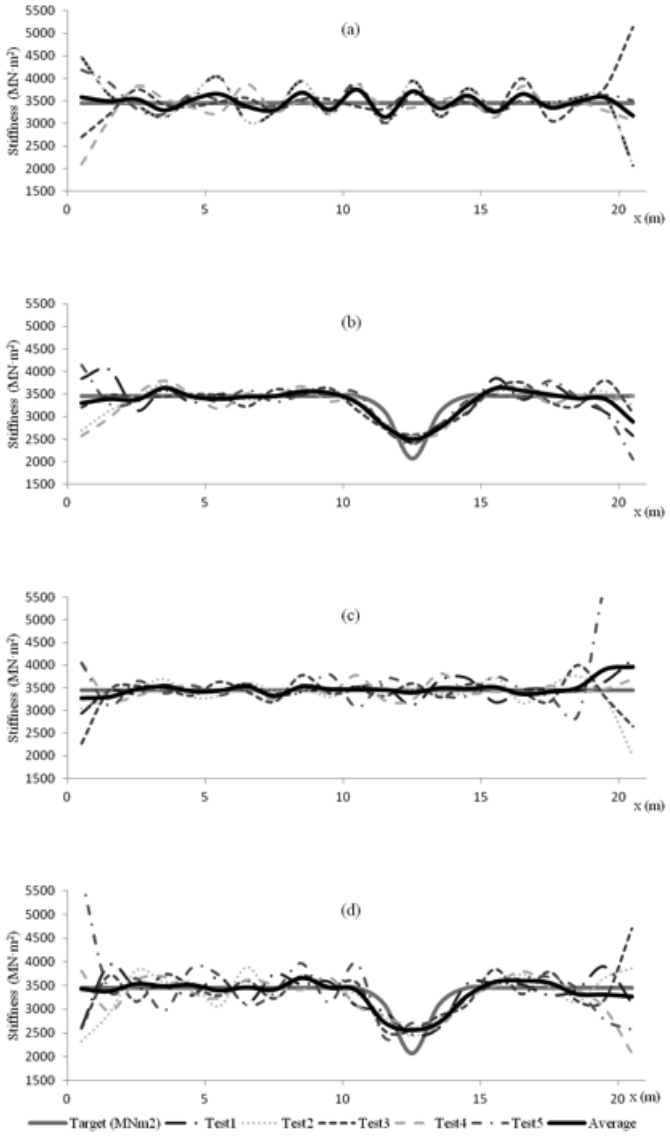


Figure 2. Target and estimated stiffness profiles using noise-free deflection measurements: (a) 10 measurements/m in a healthy beam, (b) 10 measurements/m in a damaged beam, (c) 50 measurements/m in a healthy beam, (d) 50 measurements/m in a damaged beam.

An increase in measurement density from 10 (Fig. 2a) to 50 measurements/m (Fig. 2c) improves the estimation of stiffness distribution in a healthy beam of uniform stiffness (i.e., leading to a smoother and closer profile to the target). However, no significant differences appear in the stiffness estimation of the damaged beam when using 10 (Fig. 2b) or 50 measurements/m (Fig. 2d). As it has been previously noticed (Walsh & Gonzalez, 2009; Gonzalez et al. 2013), stiffness predictions for the elements closest to the supports are unreliable due to the low sensitivity of deflection to the stiffness of these areas. Measured rotations are included as additional inputs to the CE algorithm to check their impact on the estimated stiffness (Fig. 3). A small improvement is noticeable in the results of the healthy beam, i.e., the profile in Figure 3a being smoother and closer to the target value than in Figure 2a.

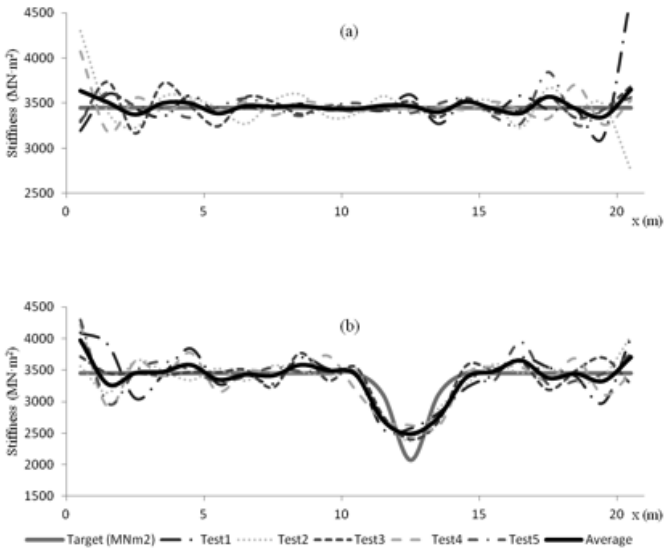


Figure 3. Estimated stiffness profiles using 10 measurements/m including displacements and rotations: (a) healthy beam, (b) damaged beam.

### 5.2 *Noisy simulations*

Noise is taking into account following the modelling procedure of Section 4.3 and it depends on the location and precision of the equipment being simulated (TAC or HDS).

When simulated TAC measurements are considered (10 measurements/m), the CE algorithm generally shows that the stiffness drops close to damaged elements (between 12 and 13 m) as shown by Figure 4, but drops can also be found in healthy elements. Therefore it could be said that the predictions by the CE algorithm are inconclusive for this particular structure and loading.

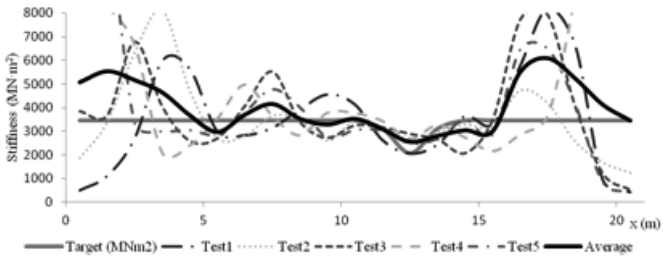

Figure 4. Target and estimated stiffness profiles using simulated TAC measurements from damaged beam.

Simulated HDS measurements (50 measurements/m) leads to higher deviations with respect to the target stiffness profiles than TAC measurements as a consequence of higher noise associated to this measuring device.

If simulated noisy rotations are included together with displacements in the CE calculations, there is not an improvement in the estimated profiles with respect to Figure 4.

Finally, several different values of deflection errors are tested, with the aim of establishing the noise limit acceptable for accurate stiffness prediction using CE in a structure of characteristics and loading similar to the one described in Section 4.2.

A simplified noise model, where all points are attributed the same maximum measurement error is adopted. Figure 5 illustrates the ability of the CE algorithm to predict damage for various deflection errors. The noise limit to identify the stiffness profile with reasonable degree of accuracy varies in a threshold between 0.4 mm and 0.8 mm. Beyond 0.8 mm, damage is not unambiguously identified.

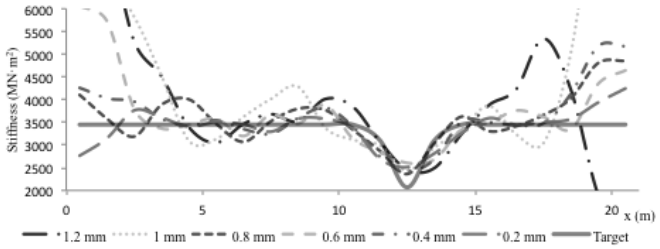


Figure 5. Target and estimated stiffness profiles (average of 5 simulations) using corrupted deflection measurements for various deflection errors and 10 measurements/m in a damaged beam.

It must be noticed that the noise limit previously recommended has been determined for a specific structure (geometry, boundary conditions and element mechanical properties), loading conditions and set of CE parameters. This noise limit may clearly be increased for more flexible structures (or larger loads) leading to higher displacements or decreased for stiffer structures (or smaller loads) leading to smaller displacements.

## 6 CONCLUSIONS

The interest of using surveying measurements for structural assessment as opposed to other sensors that need direct contact with to the structure is beyond any doubt. This paper has used simulated deflection and rotation surveying measurements to assess the accuracy of a CE algorithm in estimating the stiffness profile of a structure. For this purpose, sources of error related to the equipment (TAC and HDS) used to collect static measurements have been quantified. For the selected structure (21 m simply supported bridge) and loading case (self-weight + 2-axle truck), the CE algorithm has shown to be reliable when applied to noise-free data, using measurement *densities* of 10 (TAC) and 50 (HDS) points per meter. However, the corruption of the displacements by noise associated to TAC or HDS measurements has prevented the accurate estimation of the stiffness profiles by the CE algorithm.

The noise limit that would allow reliable stiffness profiles and to detect damage through the CE algorithm is not achievable under the test conditions in this paper. Further developments in surveying techniques appear to be necessary to achieve an adequate prediction of structural parameters using CE and static measurements as inputs. It should be noted that accuracy of deflection and rotation measurements might be higher in a real case than in the preliminary analysis carried out in this paper. Noise can be reduced through the use of higher precision tachymeters or digital levels, or through the application of sophisticated filtering algorithms to the HDS measurements. Therefore, more flexible structures or higher loads will lead to larger displacements

where noise will affect stiffness estimations to a lesser extent.

## ACKNOWLEDGMENTS

The authors wish to express their gratitude for the support received for Scientific Research under Grant No. BIA2011-26915, from the "Programa Nacional de Proyectos de Investigación Fundamental, VI Plan Nacional de Investigación Científica, Desarrollo e Innovación Tecnológica 2008-2011" of the Spanish Government towards this investigation.

## REFERENCES

Abdo, M. 2011. Parametric study from static response in structural damage detection. *Engineering Structures* 34: 124-131.

Bakhtiari-Nejad, F., Rahai, A. & Esfandiari, A. 2005. A structural damage detection method using static noisy data. *Engineering Structures* 27(12): 1784-1793.

Banan, M. R., Banan, M. R., and Hjelmstad, K. D. 1994a. Parameter estimation of structures from static response. Part I: computational aspects. *Journal of Structural Engineering* 120(11): 3243-3258.

Banan, M. R., Banan, M. R., and Hjelmstad, K. D. 1994b. Parameter estimation of structures from static response. Part II: numerical simulation studies. *Journal of Structural Engineering* 120(11): 3259-3283.

BIMP (Bureau International des Poids et Mesures). 2008. E*valuation of measurement data - Guide to the expression of uncertainty in measurement*. Paris (France): Joint Committee for Guides in Metrology.

BIMP (Bureau International des Poids et Mesures). 2012. *International vocabulary of metrology – Basic and general concepts and associated terms (VIM)*. 3rd edition. Paris (France): Joint Committee for Guides in Metrology.

Boehler, W. & Marbs, A. 2004. *Investigating Laser Scanner Accuracy*. i3mainz, Institute for Spatial Information and Surveying Technology, FH Mainz, University of Applied Sciences, Mainz, Germany. On line: http://scanning.fh-mainz.de.

Caddemi, S. & Morassi, A. 2007. Crack detection in elastic beams by static measurements. *International Journal of Solids and Structures* 44: 5301-5315.

Cheng Penggen, Shi Wenzhong & Zheng Wanxing. 2002. Large Structure Health Dynamic Monitoring Using GPS Technology. *Engineering Surveys for Construction Works and Structural Engineering FIG XXII International Congress; Washington, DC (USA), 19-26 April 2002*.

Covián, E. & Puente, V. 2013. *Fundamentos del ajuste de observaciones topográficas*. Oviedo (Spain): Publication Office of the Oviedo University.

Ghiliani, P. & Wolf, R. 2006. *Adjustment computations. Spatial data analysis*. New Jersey (USA): John Wiley & Sons.

González, A., Covián, E., Casero, M. & Cooper, J. 2013. Experimental Testing of a Cross-Entropy Algorithm to Detect Damage. *10th International Conference on Damage Assessment of Structures. Dublin (Ireland), 8-10 July 2013*.

Gordon, S.J. & Lichti, D. 2007. Modeling Terrestrial Laser Scanner Data for Precise Structural Deformation Measurement. *Journal of Surveying Engineering* 133-2: 72-80.

Hjelmstad, K. & Shin, S. 1997. Damage detection and assessment of structures from static response. *Journal of Engineering Mechanics* 123(6): 568-576.

International Organization for Standardization (ISO). 2001. *ISO 17123, Optics and optical instruments — Field procedures for testing geodetic and surveying instruments*. Geneve (Switzerland): ISO copyright office.

Li, X. Ge, L., Ambikairajah, E., Rizos, C., Tamura, Y. & Yoshida, A. 2006. Full-scale structural monitoring using an integrated GPS and accelerometer system. *GPS Solutions* 10: 233–247.

Luis, de, J.M. 2009. *Contraste en la ejecución de auscultaciones geodésicas por métodos clásicos y con láser escáner*. Tesis doctoral, Departamento de Ingeniería Geográfica y Expresión Gráfica, Cantabria University, Santander (Spain)

Marchamalo, M., Galán, D., Sánchez, J.A. & Martínez, R. 2011. La tecnología DGPS en la construcción: control de movimientos en grandes estructuras. *Informes de la Construcción* 63-522: 93-102.

Mills, J. & Barber, D. 2004. Geomatics Techniques for Structural Surveying. *Journal of Surveying Engineering* 130-2: 56-64.

Olalla Marañón, C. 2007. Auscultación de laderas. *Jornadas técnicas sobre estabilidad de laderas en embalses, Confederación Hidrográfica del Ebro, Zaragoza (Spain) June 2007*.

Psimoulis, P.A., Pytharouli, P. & Stiros, S. 2006. Experimental monitoring of oscillations of major flexible structures using GPS and RTS. *3rd IAG / 12th FIG Symposium. Baden (Austria) 22-24 May 2006*.

Sanayei, M. & Scampoli, S. 1991. Structural element stiffness identification from static test data. *Journal of Engineering Mechanics* 117(5): 1021-1036.

Walsh, B.J. & Gonzalez, A. 2009. Assessment of the condition of a beam using a static loading test. *Key Engineering Materials* 413-414: 269-276.

Wang, X., Hu, N., Hisao Fukumaga & Yao, Z.H. 2001. Structural damage identification using static test data and changes in frequencies. *Engineering Structures* 23: 610-621.

Yan, Y.J., Cheng, L., Wu, Z. Y. & Yam, L.H. 2007. Development in vibration-based structural damage detection technique. *Mechanical Systems and Signal Processing* 21: 2198-2211.

Yang, Q. & Sun, B. 2010. Structural damage localization and quantification using static test data. *Structural Health Monitoring* 10(4): 381-389.